Industrial Surface Defect Detection Method Based On Multi- Scale Feature Enhancement And Static-Dynamic Graph Relationship Modeling

Yingjie Guo

Department of Information Technology, Shanxi Professional College of Finance, Shanxi, aiyuan 030008, China

Corresponding author. E-mail: yingjiet7r@163.com

Received: May 20, 2026; Accepted: July 13, 2026

Finding industrial surface flaws is essential to ensuring production safety and manufacturing quality. However, flaws in real-world industrial settings frequently exhibit traits such as large-scale changes, complex forms, high background similarity, and inadequate sample labeling, which pose serious obstacles to automated identification. This research suggests an industrial defect detection technique that combines static-dynamic graph relationship modeling with multi-scale feature improvement to address these problems. This method introduces multi-scale dilated convolution in the feature extraction stage to balance local details with global contextual information, and combines a channel-space attention mechanism to adaptively highlight defect-related features and suppress background interference. To further enhance the model's discriminative stability and generalization capacity, a static-dynamic graph joint category relationship modeling module is built in a high-level semantic space to describe the structural relationships and dynamic similarities between defect categories. On several publicly accessible industrial defect datasets, experimental results demonstrate that the suggested approach outperforms current approaches in terms of detection performance. The proposed AM-GCN achieves 94.0% AUROC (DAGM 2007) and 90.1% mAP (NEU-DET), outperforming baselines by 0.9% and 1.9%, showing clear improvement from static–dynamic GNN modeling. Concurrently, interpretability research confirms that the model's concentration on critical fault regions during the decision-making process is more rational and focused, indicating strong engineering application potential.

Keywords: Industrial defect detection; Multi-scale features; Attention mechanism; Graph neural network; Industrial vision

http://dx.doi.org/10.6180/jase.202611_34.058

1. Introduction

As manufacturing advances toward automation, surface inspection is vital for ensuring product safety and reliability [1]. Defects in industries such as aerospace and electronics can impact performance and safety, making accurate detection a key research focus [2]. Manual inspection under long-term conditions is slow and prone to errors due to human subjectivity [3]. Industrial systems require reliable fault detection to reduce downtime and improve efficiency. Accurate anomaly detection enhances production reliability. CNN-based deep learning has improved industrial defect detection via end-to-end feature learning [4]. However, small defect size, irregular shapes, and background similarity make detection challenging [5]. Limited data reduces generalization and increases overfitting risk.

As shown in Fig. 1, industrial surface defects include stain and texture types. Stain defects appear as localized color or brightness changes, while texture defects involve structural damage such as scratches and cracks. Their differences in scale, distribution, and saliency make single-scale or single-feature methods insufficient for detection.

Several deep learning-based methods have been proposed for industrial defect detection [6], including super-

Fig. 1. Examples of stain and texture defects on industrial surfaces.

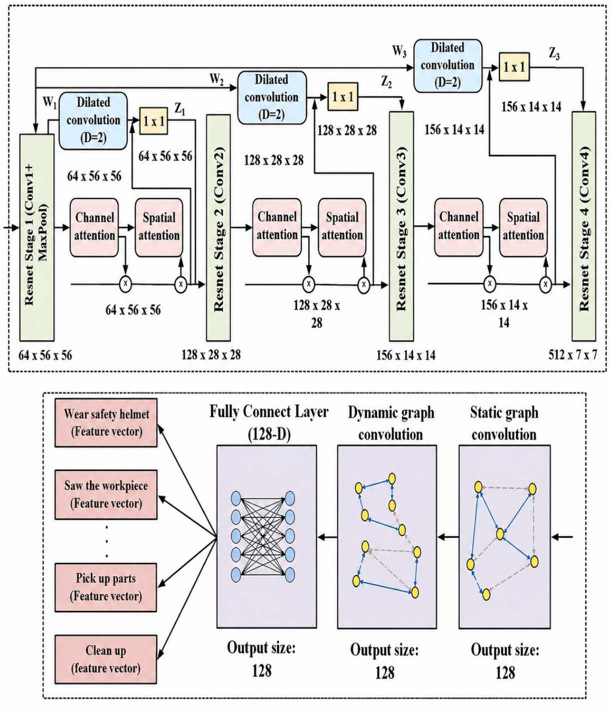

Fig. 2. Architecture of the proposed industrial anomaly detection model.

vised, weakly supervised, and unsupervised approaches. Supervised methods achieve high accuracy with sufficient labeled data [7], but data collection and annotation are costly. Recent studies have applied deep learning, attention, and graph learning for maintenance analysis. However, complex defect patterns remain challenging to model accurately. Existing methods use multi-scale features and attention mechanisms to improve defect detection and suppress background noise [8]. Some also apply GNNs for relationship modeling. However, most approaches focus on single aspects and lack joint integration, limiting overall performance.

Industrial defect detection faces challenges like scale variation, complex backgrounds, ignored category relations, and limited data. This paper proposes a multi-scale feature enhancement with category relationship modeling using dilated convolutions and attention to improve defect representation and reduce background interference.

2. Theory and formula

2.1. The Proposed Industrial Anomaly Detection Model

Fig. 2 shows the proposed framework, which enhances feature representation and category discrimination for robust industrial anomaly detection.

2.2. Feature Extraction Module

Industrial anomalies vary in size, shape, and texture, so single-level features may miss small or complex defects. Hence, a ResNet multi-stage backbone (Stage 1–Stage 4) is used to extract hierarchical features. Shallow features capture edges and textures, while deep features encode semantic and contextual information, together forming a multi-scale basis for anomaly modeling.

2.3. Reasons for introducing multi-scale dilated convolution

Industrial anomalies often vary in scale but maintain structural continuity [9]. Traditional pooling-based convolution can lose spatial details, reducing sensitivity to small defects [10]. Therefore, dilated convolutions (D=2, 3, 4) are used across ResNet stages to expand the receptive field while preserving feature resolution.

$$\mathrm{F_i}^{\mathrm{d}}(\mathrm{p}) = \sum_{k} \mathrm{W_i}(\mathrm{k}) \cdot \mathrm{F_i}\,(\mathrm{p} + \mathrm{r_i} \cdot \mathrm{k}) \tag{1}$$

This design captures both local details and global context, making it effective for detecting scale-varying industrial anomalies. Multi-scale dilated convolutions enable adaptive receptivefield learning to capture both fine-grained defect details and large-scale contextual information. This improves anomaly representation across varying defect morphologies and heterogeneous industrial surface textures.

2.4. Motivation for Joint Modeling of Channel Attention and Spatial Attention

Industrial images contain complex backgrounds, noise, and texture interference, where not all features are equally useful [11]. Therefore, cascaded channel and spatial attention is used to highlight anomaly-related features [12]. Channel attention evaluates the importance of each channel using global statistical information:

$$\mathrm{M_c} = \sigma\left(\mathrm{MLP}\left(\mathrm{GAP}\left(\mathrm{F_i^d}\right)\right)\right) \tag{2}$$

And the features are weighted:

$$\mathrm{F_i^c} = \mathrm{M_c} \odot \mathrm{F_i^d} \tag{3}$$

This mechanism enhances anomaly-relevant feature channels while suppressing noise. Spatial attention is then applied to locate abnormal regions in the image:

$$\mathrm{M_s} = \sigma\left(\mathrm{Conv}\,7\times7\left(\left[\mathrm{AvgPool}\left(\mathrm{F_i^c}\right);\mathrm{MaxPool}\left(\mathrm{F_i^c}\right)\right]\right)\right) \tag{4}$$

$$\mathrm{F_i^s} = \mathrm{M_s} \odot \mathrm{F_i^c} \tag{5}$$

By focusing on salient spatial regions, the method reduces background interference. It applies a sequential channel-spatial attention strategy for feature screening and localization.

2.5. 1×1 Convolution Alignment and Multi-Scale Feature Fusion

Features from different stages have varying channel dimensions and semantic levels, making direct fusion inconsistent. Therefore, 1×1 convolution is used to align and compress features.

$$\mathrm{Z_i} = \mathrm{Conv}\,1\times1\left(\mathrm{F_i^s}\right) \tag{6}$$

This reduces computational complexity and enables effective multi-scale feature fusion in a unified space for compact representation in class relationship modeling. The 1×1 convolution preserves essential semantic information while aligning feature dimensions, enabling effective cross-scale feature aggregation and improving consistency in hierarchical defect learning.

3. experimental setup

3.1. Category Relationship Discrimination Module

3.1.1. The necessity of introducing category relationship modeling

Industrial defects are often correlated, and ignoring these relationships may reduce classification stability [13]. Therefore, a static GCN with an adjacency matrix A_s is used to model category relationships.

$$H_s^{(l+1)} = \sigma\left(D_s^{-\frac{1}{2}} A_s D_s^{-\frac{1}{2}} H_s^{(l)} W_s^{(l)}\right) \tag{7}$$

The static graph captures stable category relations, while the dynamic graph adaptively models changing relationships using feature similarity. The dynamic adjacency matrix is defined as:

$$A_d(i,j) = \mathrm{softmax}\left(\frac{X_i^\top X_j}{|X_i|\left|X_j\right|}\right) \tag{8}$$

Dynamic graphs can adaptively adjust class relationships based on sample features, giving the model stronger scene adaptability. Finally, by fusing static and dynamic graph features:

$$\mathrm{H} = \alpha \mathrm{H_s} + (1-\alpha)\mathrm{H_d} \tag{9}$$

The anomaly category is determined through a fully connected layer, thereby enabling accurate identification of industrial anomalies.

4. Attention enhancement submodule for industrial anomaly detection

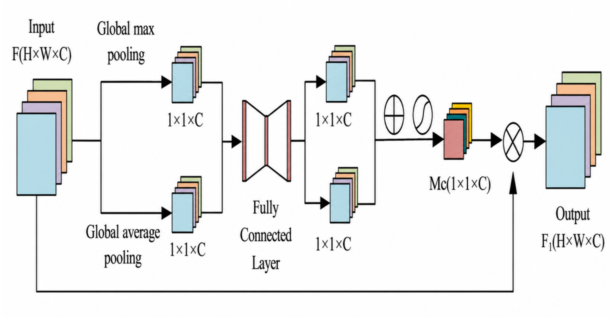

Fig. 3. Channel attention submodule.

As shown in Fig. 3, the module enhances anomaly features by suppressing background noise through attention weighting. Let the input feature map be:

$$\mathbf{F} \in \mathbb{R}^{\mathbf{H}\times\mathbf{W}\times\mathbf{C}} \tag{10}$$

Here, H, W, and C denote the feature map dimensions. Global average and max pooling are used to extract channel-wise statistics.

$$\mathrm{f_{avg}} = \mathrm{GAP}(\mathrm{F}), \quad \mathrm{f_{max}} = \mathrm{GMP}(\mathrm{F}) \tag{11}$$

Average pooling captures global trends, while max pooling highlights local anomalies for robust modeling [14]. Sigmoid activation adaptively weights features, highlighting defectrelated responses while suppressing background noise, improving anomaly representation in complex industrial scenes. The final channel attention weights are obtained through the Sigmoid function:

$$M_c = \sigma(z), \quad M_c \in \mathbb{R}^{1\times1\times c} \tag{12}$$

These weights indicate the importance of each channel for anomaly detection and are used to recalibrate the original feature map at the channel level.

5. Static–dynamic graph relationship reasoning submodule

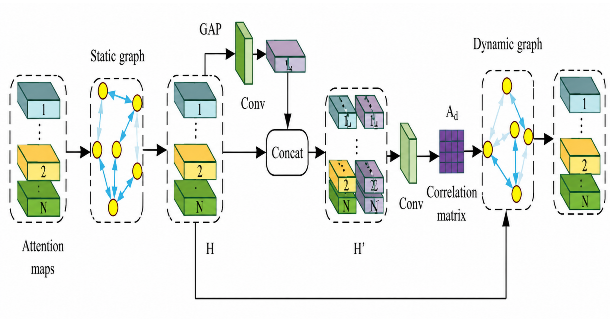

Fig. 4. Static–dynamic graph reasoning submodule.

Fig. 4 shows static and dynamic graph convolution for modeling category relationships and improving discrimination.

$$H_s^{(l+1)} = \sigma\left(D_s^{-\frac{1}{2}} A_s D_s^{-\frac{1}{2}} H_s^{(l)} W_s^{(l)}\right) \tag{13}$$

Where $\mathrm{H_s^{(0)}} = \mathrm{V}; \mathrm{D_s}$ is a degree matrix; $\mathrm{W_s^{(l)}}$ represents the learnable weights of layer (1). Static graph convolution category information, and GAP aggregates the output for further modeling.

$$\mathrm{g} = \mathrm{GAP}\left(\mathrm{H_s}\right) \tag{14}$$

As anomaly relations vary with data, static graphs are insufficient, so a dynamic correlation matrix is built from (H') :

$$A_d(i,j) = \text{softmax}\left(\frac{h_i'^{\top} h_j'}{|h_i'|, |h_j'|}\right) \tag{15}$$

Here, $\boldsymbol{h}_i'$ is the feature of the i-th category, and $\boldsymbol{A}_d$ represents the dynamic category similarity matrix. This corresponds to the correlation matrix $\boldsymbol{A}_d$.

5.1. Dynamic Graph Convolution

Perform graph convolution operations on a dynamic graph $\mathcal{G}_d$:

$$\mathrm{Z}^{(\mathrm{l}+1)} = \sigma\left(\mathrm{A_d Z^{(l)} W_d^{(l)}}\right) \tag{16}$$

Here, $\mathrm{Z}^{(0)} = \mathrm{H}'$ and $\mathrm{Z} = \mathrm{z}_1, \ldots, \mathrm{z_N}$ corresponds to $Z_1, Z_2, \ldots, Z_c$ in the graph. Dynamic graph convolution adaptively updates the class based on sample features.

6. Experiment and results analysis

6.1. Experimental Environment and Setup

6.1.1. Description of the Dataset

Two public datasets, DAGM 2007 and NEU-DET, are used for validation. DAGM 2007 contains 10 texture-based defect classes with limited samples [15] and challenging feature discrimination [16], while NEU-DET includes six annotated steel defect types for supervised detection [17].

6.1.2. Implementation details

Experiments are conducted in PyTorch [18] using a ResNet-based model with dilated convolution, attention, and graph modules [19]. Images are resized to 400×400 with data augmentation. The model is trained using the Adam optimizer for 200 epochs with a batch size 16. Proper initialization, adaptive updates, and learning-rate scheduling ensure stable convergence and efficient optimization.

6.2. Results Analysis

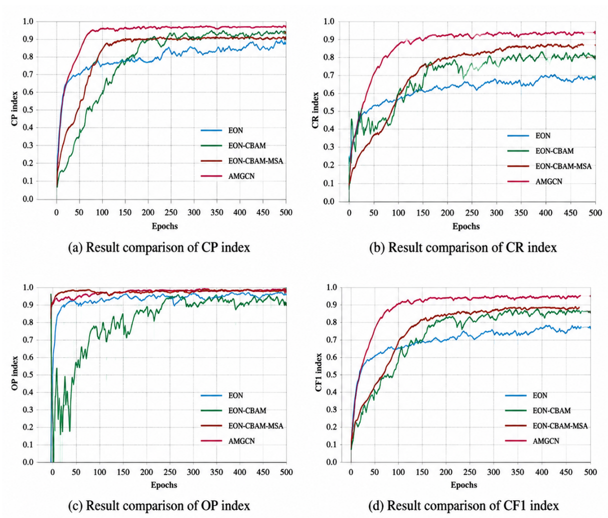

Fig. 5. The proposed framework, which enhances feature representation and category discrimination for robust industrial anomaly detection.

Fig. 5 shows that AM-GCN consistently outperforms RSN variants on CP, CR, OP, and CF1 metrics, achieving faster convergence, greater stability, and higher final performance.

Table 1 shows that AM-GCN significantly outperforms all baseline methods ($p < 0.05$), with the largest improve-

Table 1. Statistical significance analysis of AM-GCN improvements over baselines.

Comparison	AUROC Gain (%)	p -value	Significance
AM-GCN vs RSN	5.3	<0.001	Significant
AM-GCN vs RSN + CBAM	2.6	0.004	Significant
AM-GCN vs RSN + CBAM + MLS	0.9	0.018	Significant
AM-GCN vs PatchSVDD	1.9	0.009	Significant
AM-GCN vs U-Student	1.5	0.012	Significant

Table 2. AUROC with Confidence Intervals.

Method	Mean AUROC (%)	Std. Dev.	95% Confidence Interval
RSN	88.7	0.92	88.13-89.27
RSN + CBAM	91.4	0.71	90.96-91.84
RSN + CBAM + MLS	93.1	0.58	92.74-93.46
AM-GCN	94.0	0.41	93.75-94.25

ment over RSN, demonstrating its effectiveness and reliability.

Table 2 shows that AM-GCN achieves the highest AUROC with the lowest variance and a narrow 95% confidence interval, demonstrating stable, reliable, and robust performance. Fig. 6 shows that AM-GCN achieves the highest

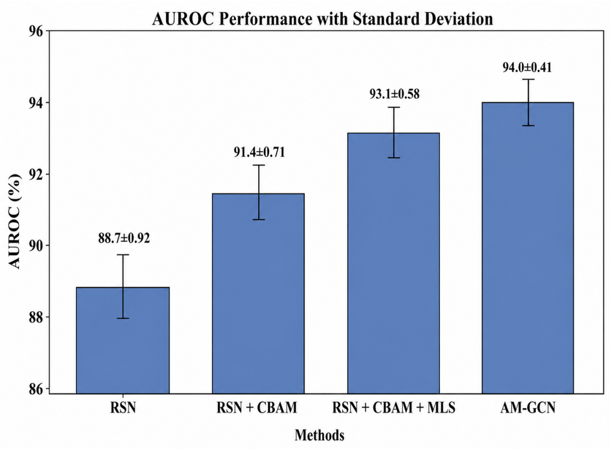

Fig. 6. AUROC Performance Comparison with Standard Deviation Across Methods.

AUROC with the lowest standard deviation, indicating superior, stable, and robust performance compared to other methods. Table 3 compares methods on DAGM and NEU-DET, showing steady gains with added modules. AM-GCN performs best with the highest accuracy and lowest variance.

Here, ↑ indicates that the larger the value, the better the performance. The spatial feature refinement module enhances fine-grained defect representation using multi-scale receptive fields. Small kernels preserve subtle structural details, while larger kernels capture broader contextual information. This combination improves robustness in microscopic defect detection. To validate each module, components are progressively added or removed in the AM-GCN framework, as shown in Table 4.

Tables 3 and 4 show that AM-GCN achieves superior performance on DAGM 2007 and NEU-DET. The results confirm that MLS, attention, and static–dynamic graph modeling effectively improve defect detection and class discrimination. The ablation study shows that dilated convolution and attention both improve defect representation, and their combination further enhances detection performance across both datasets, as shown in Table 5.

The static-dynamic graph convolution module adds minimal overhead while maintaining efficient inference. Table 6 highlights its balanced accuracy–efficiency trade-off, demonstrating suitability for industrial inspection.

Multi-scale enhancement adds minimal overhead while preserving efficiency, and dynamic graph convolution improves robustness under noisy conditions. Table 7 shows stable performance across reduction ratios, with the best result at 16. Fig. 7 shows that the proposed model accurately localizes and classifies industrial defects, demonstrating robust performance through multi-scale features, attention mechanisms, and graph-based modeling.

Fig. 8 shows accurate defect localization, effective background suppression, and improved robustness, supported by SHAP-based interpretability. Experimental results show improved detection accuracy and classification stability. The framework effectively handles complex backgrounds and diverse defect characteristics. SHAP results show the model focuses on true defect regions while suppressing background noise, validating multi-scale and attention effectiveness. Transformer backbones further improve representation and generalization, confirming the adaptability of the graph-enhanced framework across feature extractors.

Table 3. Overall performance (%) of different methods on two industrial defect datasets.

Method	Composition module	DAGM AUROC (%)	DAGM F1 (%)	NEU-DET mAP (%)	NEU-DET Recall (%)
GANomaly	refactor	76.2 ± 1.32	68.4 ± 1.15	71.3 ± 1.28	69.5 ± 1.20
1-NN	distance metric	83.9 ± 1.08	74.6 ± 0.96	78.4 ± 1.02	75.2 ± 0.94
DOCC	One type of classification	87.9 ± 0.95	78.1 ± 0.88	81.6 ± 0.91	79.4 ± 0.83
PatchSVDD	Patch characterization	92.1 ± 0.67	83.7 ± 0.61	85.9 ± 0.65	83.2 ± 0.60
U-Student	Teacher - Student	92.5 ± 0.63	84.1 ± 0.58	86.3 ± 0.61	84.0 ± 0.57
RSN	Baseline CNN	88.7 ± 0.92	80.3 ± 0.81	83.4 ± 0.86	81.1 ± 0.79
RSN + CBAM	attention	91.4 ± 0.71	83.2 ± 0.64	86.1 ± 0.69	84.0 ± 0.61
RSN + CBAM + MLS	multi-scale	93.1 ± 0.58	85.6 ± 0.52	88.2 ± 0.55	86.5 ± 0.49
AM-GCN	MLS + Attention + GCN	94.0 ± 0.41	87.3 ± 0.35	90.1 ± 0.38	88.6 ± 0.32

Table 4. Component analysis results (AM-GCN module ablation, %).

Model variants	Multiscale (MLS)	Attention (CA+SA)	Diagram Relationships (GCN)	DAGM AUROC	NEUDET mAP
Baseline (RSN)	X	X	X	88.7	83.4
+ MLS	√	X	X	90.6	85.0
+ MLS + Attention	√	√	X	92.8	87.1
+ MLS + Static-GCN	√	×	√	91.9	86.2
+ MLS + DynamicGCN	√	X	√	92.3	86.8
AM-GCN (Full)	√	√	√	94.0	90.1

Table 5. Focused Ablation Study on Attention and Dilated Convolution Modules.

Model Variants	Dilated Convolution (MLS)	Attention (CA + SA)	DAGM (%) AUROC (%)	NEU-DET mAP (%)
Baseline (RSN)	X	X	88.7	83.4
+ Dilated Convolution	√	X	90.6	85.0
+ Attention Mechanism	X	√	91.4	86.1
+ MLS + Attention	√	√	92.8	87.1

Table 6. Computational Efficiency Analysis of Static-Dynamic Graph Network.

Method	Parameters (M)	FLOPs (G)	Inference Time (ms/image)	Memory Usage (MB)
ResNet Backbone	25.6	4.1	18.2	420
+ Static Graph Module	28.3	4.8	20.5	450
+ Dynamic Graph Module	29.1	5.2	21.3	465
Proposed Static-Dynamic GCN	29.8	5.5	22.1	470

Table 7. Hyperparameter sensitivity analysis of the shared MLP reduction ratio.

Reduction Ratio (r)	DAGM 2007 AUROC (%)	NEU-DET mAP (%)
4	93.4	89.1
8	93.8	89.6
16	94.0	90.1
32	93.6	89.4

7. Conclusion

This paper addresses the challenges of significant multi-scale variations, complex backgrounds, and neglected category relationships in industrial surface defect detection. It proposes a detection method that combines multi-scale feature enhancement with joint modeling of static-dynamic graph relationships. The multi-scale feature enhancement (MLS) module independently improves defect representation by capturing both fine-grained local details and global contextual information, which significantly strengthens the model's ability to detect defects of varying sizes. The proposed approach achieves reliable anomaly detection through enhanced feature learning and relationship modeling, demonstrating potential for industrial inspection. Extensive experimental results demonstrate that the pro-

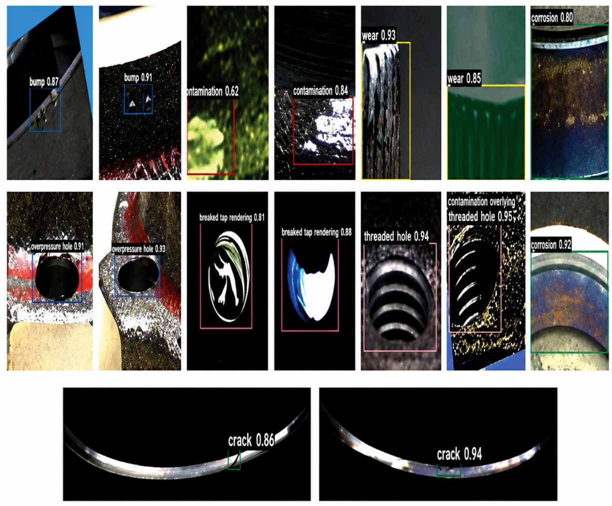

Fig. 7. Visualization of detection results on the industrial defect dataset.

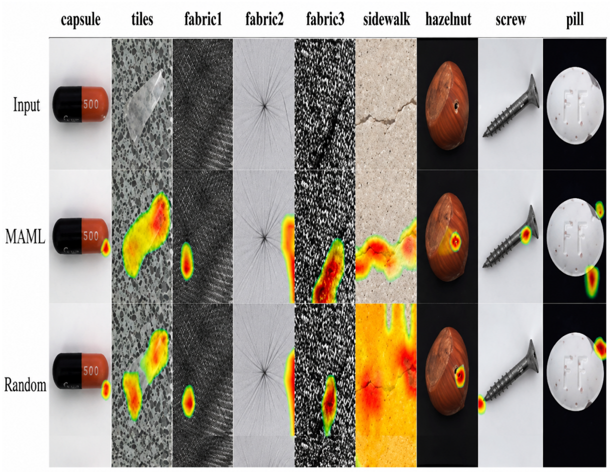

Fig. 8. Comparison of anomaly response visualization results industrial categories.

posed method outperforms existing methods in terms of detection accuracy, robustness, and small-sample adaptability. Future work will explore more efficient model structures and cross-scenario adaptive capabilities to promote the practical application of this method in real industrial production lines. Future work will explore the scalability of the proposed static–dynamic graph relationship modeling in real-time and edge-based industrial environments, with emphasis on reducing computational complexity for efficient deployment on resource-constrained devices.

References

[1] G. Fu, W. Le, Z. Zhang, J. Li, Q. Zhu, F. Niu, H. Chen, F. Sun, and Y. Shen, (2023) *"A surface defect inspection model via rich feature extraction and residual-based progressive integration"* **Machines** ***11***(1): 124. DOI: 10.3390/machines11010124.

[2] X. Jia, X. Zhou, Z. Shi, Q. Xu, and G. Zhang, (2025) *"Geoiou-sea-yolo: An advanced model for detecting unsafe behaviors on construction sites"* **Sensors** ***25***(4): 1238. DOI: 10.3390/s25041238.

[3] C. Nie, C. Zhou, T. Wang, X. Wang, H. Zhou, and H. Feng, (2025) *"Linear rolling guide surface wear-state identification based on multi-scale fuzzy entropy and random forest"* **Lubricants** ***13***(8): 323. DOI: 10.3390/lubricants13080323.

[4] H. Chen, Y. Pang, Q. Hu, and K. Liu, (2020) *"Solar cell surface defect inspection based on multispectral convolutional neural network"* **Journal of Intelligent Manufacturing** ***31***(2): 453–468. DOI: 10.1007/s10845-018-1458-z.

[5] C. Zhang, B.-H. Roh, and G. Shan. "Poster: Dynamic clustered federated framework for multi-domain network anomaly detection". In: *Companion of the 19th International Conference on Emerging Networking EXperiments and Technologies (CoNEXT 2023)*. New York: Association for Computing Machinery, 2023, 71–72. DOI: 10.1145/3624354.3630086.

[6] L. Yuan, (2025) *"Mine gas time-series data prediction and fluctuation monitoring method based on decomposition-enhanced cross-graph forecasting and anomaly finding"* **Sensors** ***25***(22): 7014. DOI: 10.3390/s25227014.

[7] Y. L. He, Z. H. Liu, W. Zhang, D. R. Dai, Z. W. Pang, M. X. Xu, and D. Gerada, (2025) *"Eccentricity fault diagnosis of permanent magnet synchronous generators based on 2D recursive fusion graph and CBAM-ConvNeXt-FPN"* **Measurement Science and Technology** ***36***(5): 056110. DOI: 10.1088/1361-6501/adcd8e.

[8] Y. Zhang, H. G. Soon, D. Ye, J. Y. H. Fuh, and K. Zhu, (2019) *"Powder-bed fusion process monitoring by machine vision with hybrid convolutional neural networks"* **IEEE Transactions on Industrial Informatics** ***16***(9): 5769–5779. DOI: 10.1109/TII.2019.2956078.

[9] X. Lv, Y. Lan, B. Wu, L. Niu, L. Li, and W. Du, (2025) *"REL-YOLO: Surface defect detection of elevator wire rope based on improved YOLOv8"* **Journal of Supercomputing** ***81***(10): 1110. DOI: 10.1007/s11227-025-07585-0.

[10] V. Sampath, I. Maurtua, J. J. Aguilar, A. Rivera-Pinto, and J. Molina, (2023) *"Attention-guided multitask learning for surface defect identification"* **IEEE Transactions on Industrial Informatics** ***19***(9): 9713–9723. DOI: 10.1109/TII.2023.3234030.

[11] J. Chen, M. Feng, and T. S. Wirjanto. "Prospective multi-graph cohesion for multivariate time series anomaly detection". In: *Proceedings of the Eighteenth ACM International Conference on Web Search and Data Mining*. 2025, 98–106. DOI: 10.1145/3701551.3703494.

[12] P. Patil, S. Naskar, and P. J. Guruprasad, (2025) *"Multi-scale stochastic dynamic analysis of a damaged pretwisted composite strip"* **Journal of Composite Materials *59***(6): 755–780. DOI: 10.1177/00219983241297095.

[13] J. Gao, A. P. French, M. P. Pound, Y. He, T. P. Pridmore, and J. G. Pieters, (2020) *"Deep convolutional neural networks for image-based Convolvulus sepium detection in sugar beet fields"* **Plant Methods *16***(1): 1–12. DOI: 10.1186/s13007-020-00570-z.

[14] Y. Liu, H. Pu, and D. W. Sun, (2021) *"Efficient extraction of deep image features using convolutional neural network (CNN) for applications in detecting and analysing complex food matrices"* **Trends in Food Science & Technology *113***: 193–204. DOI: 10.1016/j.tifs.2021.04.042.

[15] S. U. Jan, Y. D. Lee, and I. S. Koo, (2021) *"A distributed sensor-fault detection and diagnosis framework using machine learning"* **Information Sciences *547***: 777–796. DOI: 10.1016/j.ins.2020.08.068.

[16] C. Hu and Y. Wang, (2020) *"An efficient convolutional neural network model based on object-level attention mechanism for casting defect detection on radiography images"* **IEEE Transactions on Industrial Electronics *67***(12): 10922–10930. DOI: 10.1109/TIE.2019.2962437.

[17] S. Nosratabadi, A. Mosavi, P. Duan, P. Ghamisi, F. Filip, S. S. Band, and A. H. Gandomi, (2020) *"Data science in economics: Comprehensive review of advanced machine learning and deep learning methods"* **Mathematics *8***(10): 1799. DOI: 10.3390/math8101799.

[18] T. Cuong-Le, T. Nghia-Nguyen, S. Khatir, P. Trong-Nguyen, S. Mirjalili, and K. D. Nguyen, (2022) *"An efficient approach for damage identification based on improved machine learning using PSO-SVM"* **Engineering with Computers *38***(4): 3069–3084. DOI: 10.1007/s00366-021-01299-6.

[19] J. Zhou, D. Zhang, W. Ren, and Z. Weishi, (2022) *"Auto color correction of underwater images utilizing depth information"* **IEEE Geoscience and Remote Sensing Letters *19***: 1–5. DOI: 10.1109/LGRS.2022.3170702.